Articles

Metal–Organic Chemical Vapor Deposition of Copper and Copper(I) Oxide from Copper(I) *tert*-Butoxide

Patrick M. Jeffries,[†] Lawrence H. Dubois,*[,‡] and Gregory S. Girolami*[,†]

School of Chemical Sciences and Materials Research Laboratory, University of Illinois at Urbana-Champaign, 505 S. Mathews Avenue, Urbana, Illinois 61801, and AT&T Bell Laboratories, 600 Mountain Avenue, Murray Hill, New Jersey 07974

Received February 19, 1992. Revised Manuscript Received August 25, 1992

Metal–organic chemical vapor deposition (MOCVD) from the tetrameric precursor copper(I) *tert*-butoxide, $[Cu(O\text{-}t\text{-}Bu)]_4$, results in the deposition of pure copper(I) oxide whiskers at 510 K and of copper metal films with ~2% oxygen contamination at 670 K. Both deposits are polycrystalline as judged by X-ray powder diffraction. Quantitative analyses of the gaseous byproducts generated during the deposition of copper(I) oxide show that 1.66 ± 0.08 equiv of *tert*-butyl alcohol, 2.14 ± 0.08 equiv of isobutylene, and 0.32 ± 0.16 equiv of water are formed for every mole of $[Cu(O\text{-}t\text{-}Bu)]_4$ consumed; essentially identical product distributions are obtained for the deposition of copper metal. The mechanisms by which copper(I) oxide and copper metal are produced from copper(I) *tert*-butoxide have been established from these product distribution studies combined with the results of high-resolution electron energy loss spectroscopy and temperature-programmed desorption studies of Cu(111) single crystals dosed with copper(I) *tert*-butoxide in ultra high vacuum. Copper(I) oxide is formed by elimination of isobutylene from surface-bound *tert*-butoxide groups to yield surface hydroxide intermediates, which subsequently engage in proton transfer processes to produce *tert*-butyl alcohol and water. The deposition of copper at 670 K evidently occurs by loss of oxygen from an initially deposited copper(I) oxide phase. This latter mechanism is supported by the observation that MOCVD deposits of high surface area copper(I) oxide deoxygenate under vacuum at 670 K to give copper metal. Thus, these studies show that MOCVD-grown films of pure metals can sometimes be produced via intermediate oxide phases whose *bulk* form is kinetically stable under the same experimental conditions.

Introduction

The metal–organic chemical vapor deposition (MOCVD) of copper films and of other copper-containing phases will be of increasing importance to the electronics industry in the twenty-first century. In particular, copper may soon replace aluminum and tungsten as the metal of choice for interconnects between circuit devices.[1-3] Two problems arise as these devices and therefore interconnects become smaller and more densely packed: the maximum possible microprocessor frequency becomes limited by the impedance of the interconnects, and the structural integrity of the interconnects becomes more quickly degraded by electromigration and stress voiding. Copper offers advantages over both metals due to its lower electrical resistivity; in addition, copper offers advantages over aluminum due to its greater structural integrity. Several MOCVD methods have been developed over the last few years to deposit films of metallic copper: from β-diketonate complexes of copper(II) using thermal,[4-11] plasma enhanced,[12,13] photochemical,[14,15] or laser-induced methods,[16-18] and more recently from Lewis base adducts of copper(I) β-diketonate,[19-25] cyclopentadienyl,[26-28] and alkoxide[24] complexes.

In the longer term, high-temperature superconductors such as $YBa_2Cu_3O_7$ potentially offer even greater advantages as interconnect materials due to their zero resistance at 77 K. Many of the high-temperature superconducting phases can be deposited by MOCVD.[29-32] Copper(II) β-diketonate complexes have typically been employed as the precursors to the copper oxide components in these depositions.

[†] University of Illinois at Urbana-Champaign.
[‡] AT&T Bell Laboratories.

(1) Pai, P.; Ting, C. H. *IEEE Electron Device Letters* **1989**, *10*, 423–425.
(2) Chamberlain, M. B. *Thin Solid Films* **1982**, *91*, 155–162.
(3) Hu, C. K.; Chang, S.; Small, M. B.; Lewis, J. E. *Proc. IEEE VLSI Multilevel Interconnection Conf.* **1986**, 181–187.
(4) Van Hemert, R. L.; Spendlove, L. B.; Sievers, R. E. *J. Electrochem. Soc.* **1965**, *112*, 1123–1126.
(5) Kaloyeros, A. E.; Feng, A.; Garhart, J.; Brooks, K.; Ghosh, S.; Saxena, A.; Leuhrs, F. *J. Electron. Mater.* **1990**, *19*, 271–276.
(6) Temple, D.; Reisman, A. *J. Electrochem. Soc.* **1989**, *136*, 3525–3529.
(7) Kaloyeros, A. E.; Saxena, A. N.; Brooks, K.; Ghosh, S.; Einsenbraun, E. *Mater. Res. Soc. Symp. Proc.* **1990**, *181*, 79–85.
(8) Armitage, D. N.; Dunhill, N. I.; West, R. H.; Williams, J. O. *J. Cryst. Growth* **1991**, *108*, 683–687.
(9) Pauleau, Y.; Fasasi, A. Y. *Chem. Mater.* **1991**, *3*, 45–50.
(10) Lecohier, B.; Philippoz, J. M.; Calpini, B.; Stumm, T.; van den Bergh, H. *J. Phys. IV* **1991**, *1*, Sect C2, 279–286.
(11) Pilkington, R. D.; Jones, P. A.; Ahmed, W.; Tomlinson, R. D.; Hill, A. E.; Smith, J. J.; Nuttall, R. *J. Phys. IV* **1991**, *1*, sect C2, 263–269.
(12) Oehr, C.; Suhr, H. *Appl. Phys. A* **1988**, *45*, 151–154.
(13) Pelletier, J.; Pantel, R.; Oberlin, J. C.; Pauleau, Y.; Gouy-Pailler, P. *J. Appl. Phys.* **1991**, *70*, 3862–3866.
(14) Houle, F. A.; Wilson, R. J.; Baum, T. H. *J. Vac. Sci. Technol. A* **1986**, *4*, 2452–2458.
(15) Jones, C. R.; Houle, F. A.; Kovac, C. A.; Baum, T. H. *Appl. Phys. Lett.* **1985**, *46*, 97–99.
(16) Houle, F. A.; Jones, C. R.; Baum, T.; Pico, C.; Kovac, C. A. *Appl. Phys. Lett.* **1985**, *46*, 204–206.
(17) Moylan, C. R.; Baum, T. H.; Jones, C. R. *Appl. Phys. A* **1986**, *40*, 1–5.
(18) Markwalder, B.; Widmer, M.; Braichotte, D.; van den Bergh, H. *J. Appl. Phys.* **1989**, *65*, 2470–2474.
(19) Norman, J. A. T.; Muratore, B. A.; Dyer, P. N.; Roberts, D. A.; Hochberg, A. K. *J. Phys. IV* **1991**, *1*, sect C2, 271–278.
(20) Shin, H. K.; Chi, K. M.; Hampden-Smith, M. J.; Kodas, T. T.; Farr, J. D.; Paffett, M. *Adv. Mater.* **1991**, *3*, 246–248.

0897-4756/92/2804-1169$03.00/0

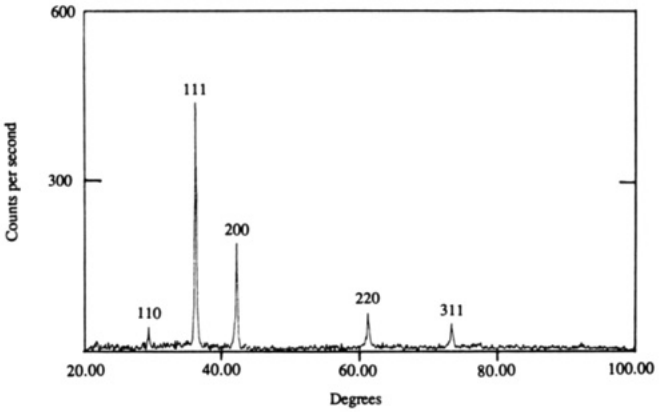

Figure 1. X-ray powder diffraction profile of copper(I) oxide deposit on borosilicate glass obtained from $[Cu(O\text{-}t\text{-}Bu)]_4$ at 510 K.

Copper oxides have also been discussed as possible low cost thin film semiconductors in the fabrication of solar cells.[33-37] Copper(I) oxide has a theoretical quantum efficiency of 12%; however, experimental efficiencies have been less than 2%.[33,34] The low experimental efficiencies are a consequence of the methods used to prepare the copper(I) oxide samples: thermal oxidation of copper metal at 1000 °C leads to films that contain structural defects,[35-37] while solution electrodeposition methods yield impure deposits.[36] A MOCVD process would therefore be of interest due to the ability of MOCVD methods to deposit high-purity and low-defect films at low temperatures.

In our preliminary communication, we reported one of the first uses of a copper(I) precursor for the chemical vapor deposition of copper-containing films by MOCVD.[38] Since that time, copper(I) precursors have been the subject of intense study.[19-28] We now describe full details of the MOCVD of copper(I) oxide and copper metal from the molecular copper(I) alkoxide, copper(I) *tert*-butoxide, $[Cu(O\text{-}t\text{-}Bu)]_4$. The phase deposited depends on the temperature, and we have accounted for this behavior by determining how the chemistry changes as the temperature is varied. An important consequence of these results is the realization that the chemical vapor deposition of pure metals can sometimes occur via metal oxide intermediates whose bulk form is kinetically stable under the same experimental conditions.

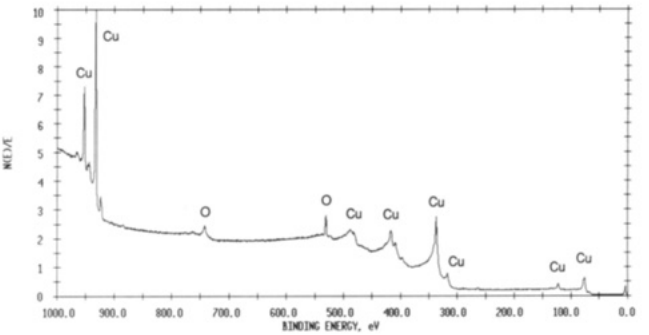

Figure 2. XPS of copper(I) oxide deposit on borosilicate glass obtained from $[Cu(O\text{-}t\text{-}Bu)]_4$ at 510 K.

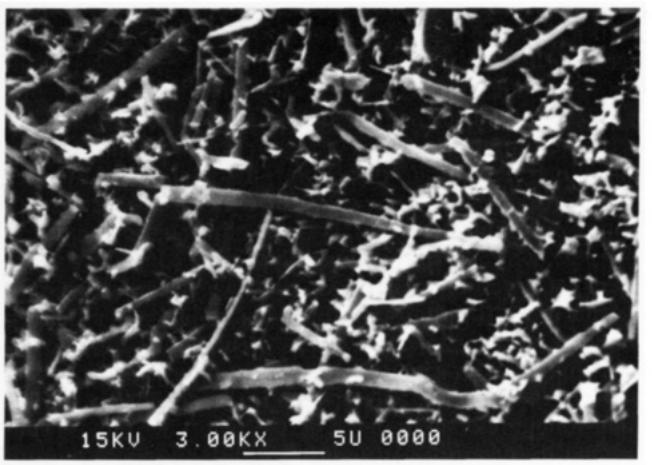

Figure 3. SEM micrograph at 15 kV showing whisker structure of copper(I) oxide deposit on borosilicate glass obtained from $[Cu(O\text{-}t\text{-}Bu)]_4$ at 510 K.

Results and Discussion

Metal alkoxides have previously been used to deposit a variety of metal oxide phases;[39,40] such precursors often lead to chemically pure deposits at reasonably low temperatures. Accordingly, we thought that it was of interest to investigate copper alkoxides as precursors for the deposition of copper-containing phases.[41] Copper(I) *tert*-butoxide, $[Cu(O\text{-}t\text{-}Bu)]_4$, is a tetramer in the solid state whose structure consists of a square-planar array of four copper atoms in which alkoxide ligands bridge each edge.[42] It is a white air-sensitive solid that sublimes at 110 °C at 10^{-4} Torr. Although its vapor pressure is thus considerably lower than many of the copper β-diketonates, particularly those with hexafluoroacetylacetonate ligands, the behavior of $[Cu(O\text{-}t\text{-}Bu)]_4$ under MOCVD conditions is quite unusual and worthy of study.

Deposition of Copper(I) Oxide. Passage of copper(I) *tert*-butoxide vapor over borosilicate glass at 510 K and ca. 10^{-4} Torr results in the formation of reddish-yellow deposits. This material gives sharp X-ray powder diffraction peaks at the proper d spacings and intensities for copper(I) oxide (Figure 1); no peaks are observed for

(21) Kumar, R.; Fronczek, F. R.; Maverick, A. W.; Lai, W. G.; Griffin, G. L. *Chem. Mater.* **1992**, *4*, 577–582.
(22) Chi, K. M.; Shin, H. K.; Hampden-Smith, M. J.; Kodas, T. T.; Duesler, E. N. *Inorg. Chem.* **1991**, *30*, 4293–4294.
(23) Chi, K. M.; Shin, H. K.; Hampden-Smith, M. J.; Duesler, E. N.; Kodas, T. T. *Polyhedron*, **1991**, *10*, 2293–2299.
(24) Hampden-Smith, M. J.; Kodas, T. T.; Paffett, M.; Farr, J. D.; Shin, H. K. *Chem. Mater.* **1990**, *2*, 636–639.
(25) Reynolds, S. K.; Smart, C. J.; Baran, E. F.; Baum, T. H.; Larson, C. E.; Brock. P. J. *Appl. Phys. Lett.* **1991**, *59*, 2332–2334.
(26) Beach, D. B.; LeGoues, F. K.; Hu, C. *Chem. Mater.* **1990**, *2*, 216–219.
(27) Beach, D. B.; Kane, W. F.; Legoues, F. K.; Knors, C. J. *Mater. Res. Soc. Symp. Proc.* **1990**, *181*, 73–77.
(28) Dupuy, C. G.; Beach, D. B.; Hurst, J. E.; Jasinski, J. M. *Chem. Mater.* **1989**, *1*, 16–18.
(29) Zhang, J. M.; Wessels, B. W.; Tonge, L. M.; Marks, T. J. *Appl. Phys. Lett.* **1990**, *56*, 976–978.
(30) Singh, R.; Sinha, S.; Hsu, N. J.; Chou, P. *J. Appl. Phys.* **1990**, *67*, 1562–1565.
(31) Zhang, K.; Boyd, E. P.; Kwak, B. S.; Wright, A. C.; Erbil, A. *Appl. Phys. Lett.* **1989**, *55*, 1258–1260.
(32) Zhang, J. M.; Marcy, H. O.; Tonge, L. M.; Wessels, B. W.; Marks, T. J.; Kannewurf, C. R. *Appl. Phys. Lett.* **1989**, *55*, 1906–1908.
(33) Rai, B. P. *Sol. Cells* **1988**, *25*, 265–272.
(34) Rakhshani, A. E. *Solid State Electron.* **1986**, *29*, 7–17.
(35) Olsen, L. C.; Addis, F. W.; Miller, W. *Sol. Cells* **1982–1983**, *7*, 247–279.
(36) Sears, W. M.; Fortin, E. *Sol. Energy Mater.* **1984**, *10*, 93–103.
(37) Weichman, F. L.; Reyes, J. M. *Can. J. Phys.* **1980**, *58*, 325–333.
(38) Jeffries, P. M.; Girolami, G. S. *Chem. Mater.* **1989**, *1*, 8–10.
(39) Bradley, D. C. *Chem. Rev.* **1989**, *89*, 1317–1322.
(40) Hough, R. L. *Proc. 3rd Int. Conf. Chem. Vap. Dep.* **1972**, 232–241.
(41) Some mixed copper(I) alkoxide/fluoroalkoxide complexes have been reported to be volatile: Gross, M. E. *J. Electrochem. Soc.* **1991**, *131*, 2422–2426.
(42) Greiser, T.; Weiss, E. *Chem. Ber.* **1976**, *109*, 3142–3146.

copper metal or copper(II) oxide. The intensities of the diffraction peaks are similar to those of powdered samples of copper(I) oxide, and thus there is no evidence of oriented growth under these conditions. X-ray photoelectron spectroscopy (XPS) confirms the composition of the deposits and establishes the absence of carbon (Figure 2).[43,44] Scanning electron microscopy (SEM) images reveal that the deposits consist of a mass of whiskers that are typically 0.5–0.75 μm thick and up to 35 μm long (Figure 3). The whiskers are not strongly adherent and can be removed easily from the substrate.

These results represent the first thermal MOCVD route to pure copper(I) oxide; a chemical vapor transport method[45,46] and an argon/oxygen plasma enhanced MOCVD method[47] using bis(2,4-pentanedionato)copper(II) have also been reported. Although $[Cu(O\text{-}t\text{-}Bu)]_4$ can produce pure copper(I) oxide at low temperatures by MOCVD, it is unlikely that this precursor would be useful on an industrial scale for deposition of copper(I) oxide photovoltaics due to its rather low volatility compared to some other copper metal precursors.

Organic Byproducts Formed during Copper(I) Oxide Deposition. To determine the mechanism by which copper(I) oxide is deposited from $[Cu(O\text{-}t\text{-}Bu)]_4$, it is first necessary to establish the byproducts formed and to quantify the amounts produced. The byproduct gases exiting the deposition zone were sampled during a MOCVD run, and quadrupole mass spectroscopic analyses indicated that *tert*-butyl alcohol and isobutylene are the *only* detectable organic byproducts. The formation of these two species is consistent with previous studies of the decomposition of other metal *tert*-butoxide complexes.[39,48–50] Small amounts of water also appeared in the mass spectra, but because water is a background contaminant that is always present, it is difficult to establish whether this species is also a product of the MOCVD process.

Because the depositions are performed under a dynamic vacuum, it is not possible to use the quadrupole mass spectrometer to quantify the exact amounts of *tert*-butyl alcohol and isobutylene formed. Accordingly, studies were carried out in a *closed* static system so that the gaseous byproducts could be collected and analyzed quantitatively. The apparatus used to perform these experiments (described in detail in the experimental section) allows the collection of the byproducts in an NMR tube as they are formed. The byproducts were sealed in the NMR tube along with a deuterated solvent and a known amount of an integration standard.

Under a static vacuum with the precursor reservoir heated to 380 K and the deposition zone heated to 510 K, thermolysis of the precursor occurs over 12 h to form principally copper(I) oxide as shown by elemental analyses. Quantitative ^1H NMR spectroscopy shows that 1.66 ± 0.08 equiv of *tert*-butyl alcohol and 2.14 ± 0.08 equiv of isobutylene are formed per equiv of $[Cu(O\text{-}t\text{-}Bu)]_4$ consumed. The amounts of *tert*-butyl alcohol and isobutylene generated account for 95% of the carbon originally present in the precursor. No other organic products were detected above the limits of sensitivity of the NMR technique (<2%).

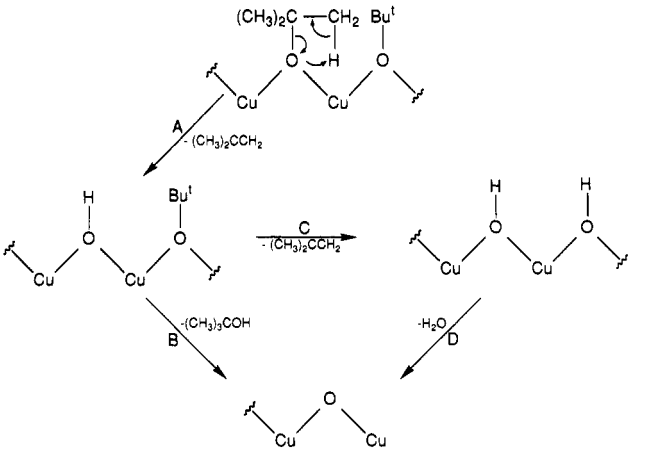

Figure 4. Elimination mechanism proposed for the deposition of copper(I) oxide from $[Cu(O\text{-}t\text{-}Bu)]_4$.

Mechanism of Copper(I) Oxide Deposition. At least two pathways can account for the deposition of copper(I) oxide and the formation of *tert*-butyl alcohol and isobutylene. The first possible mechanism is a hydrolysis/dehydration sequence (eqs 1 and 2), in which water desorbs from the glass walls of the MOCVD apparatus during deposition and participates in the deposition process. In this mechanism, isobutylene is produced in a second step by dehydration of the primary hydrolysis product *tert*-butyl alcohol. A similar mechanism has been proposed for the decomposition of $Zr(O\text{-}t\text{-}Bu)_4$ in a closed constant-pressure system.[39,48,49] In fact, the dehydration of alcohols including *tert*-butyl alcohol has been shown to be catalyzed by certain transition metals and metal oxides.[51,52]

$$[CuOC(CH_3)_3]_4 + 2H_2O \rightarrow 2Cu_2O + 4HOC(CH_3)_3 \quad (1)$$

$$HOC(CH_3)_3 \rightarrow CH_2{=}C(CH_3)_2 + H_2O \quad (2)$$

If the hydrolysis/dehydration mechanism is operative, then substantial dehydration of *tert*-butyl alcohol must occur under MOCVD conditions to account for the significant amount of isobutylene observed. Accordingly, control experiments under static and dynamic conditions were carried out by passing *tert*-butyl alcohol over heated fresh deposits of copper(I) oxide and copper metal that had been generated by MOCVD from $[Cu(O\text{-}t\text{-}Bu)]_4$. In *no* cases were detectable amounts of isobutylene generated. Thus, the hydrolysis/dehydration mechanism cannot account for the significant amount of isobutylene formed under our reaction conditions and can be ruled out on this basis.

A second possible mechanism is an elimination reaction in which isobutylene and *tert*-butyl alcohol are formed directly from surface-bound *tert*-butoxide groups. In the simplest form, this mechanism can be represented by eqs 3 and 4. In the first step, *tert*-butoxide ligands eliminate isobutylene and leave behind surface hydroxyl groups; in the second step transfer of hydroxyl protons to nearby *tert*-butoxide groups yields *tert*-butyl alcohol. A similar mechanism has been proposed for the decomposition of

$$[CuOC(CH_3)_3]_4 \rightarrow Cu_4(OH)_2[OC(CH_3)_3]_2 + 2CH_2{=}C(CH_3)_2 \quad (3)$$

$$Cu_4(OH)_2[OC(CH_3)_3]_2 \rightarrow 2Cu_2O + 2HOC(CH_3)_3 \quad (4)$$

(43) McIntyre, N. S.; Cook, M. G. *Anal. Chem.* **1975**, *47*, 2208–2213.
(44) *Handbook of X-ray Photoelectron Spectroscopy*; Muilenberg, G. E., Ed.; Perkin-Elmer: Eden Prarie, MN, 1978; p 82.
(45) Krabbes, G.; Opperman, H. *Krist. Technol.* **1977**, *12*, 929–939.
(46) Krabbes, G.; Opperman, H. *Krist. Technol.* **1977**, *12*, 1099–1104.
(47) Holzschuh, H.; Suhr, H. *Appl. Phys. A* **1990**, *51*, 486–490.
(48) Bradley, D. C.; Faktor, M. M. *J. Appl. Chem.* **1959**, *9*, 435–439.
(49) Bradley, D. C.; Faktor, M. M. *Trans. Faraday Soc.* **1959**, *55*, 2117–2123.
(50) Nandi, M.; Rhubright, D.; Sen, A. *Inorg. Chem.* **1990**, *29*, 3065–3066.
(51) Schächter, K.; Tétényi, P. *Acta Chim. Acad. Sci. Hung.* **1965**, *46*, 229–240.
(52) Tétényi, P.; Schächter, K. *Acta Chem. Acad. Sci. Hung.* **1968**, *56*, 141–152.

$Ti(O\text{-}t\text{-}Bu)_4$ under flash vacuum pyrolysis conditions.[50]

Although equal amounts of *tert*-butyl alcohol and isobutylene might be expected from an elimination mechanism, the quantitative results clearly show that the isobutylene to *tert*-butyl alcohol ratio is significantly larger than 1:1. It has already been established from control experiments that the excess isobutylene cannot be the result of in situ dehydration of *tert*-butyl alcohol. Instead, the product distribution can be accounted for by the sequence of steps shown in Figure 4. Surface *tert*-butoxide groups can eliminate isobutylene to form hydroxide species (step A), and subsequent proton transfer to nearby copper *tert*-butoxide groups yields *tert*-butyl alcohol (step B). Alternatively, nearby *tert*-butoxide groups can eliminate isobutylene (step C) and subsequent proton transfer from one hydroxide species to another yields water (step D). In both cases, the metal-containing product is copper(I) oxide. Whereas equal amounts of *tert*-butyl alcohol and isobutylene would be produced if only steps A and B were operative, steps C and D account for the larger amount of isobutylene formed.

This view of the deposition mechanism predicts that one equivalent of water should be formed for every equivalent of *excess* isobutylene produced; thus, the overall decomposition reaction could be written as eq 5, where x would

$$[CuOC(CH_3)_3]_4 \rightarrow 2Cu_2O + (2 + x)CH_2{=}C(CH_3)_2 + (2 - x)HOC(CH_3)_3 + xH_2O \quad (5)$$

equal ca. 0.26 based on the experimentally observed isobutylene to *tert*-butyl alcohol ratio. If water is formed, it would not be detected as a separate peak in the NMR spectrum of the collected byproducts due to rapid exchange of the protons of water with the hydroxyl protons of *tert*-butyl alcohol. Careful integration of the ^1H NMR spectrum shows that the ratio of the OH to $C(CH_3)_3$ peaks of *tert*-butyl alcohol is 1.4:9 rather than 1:9. The extra intensity in the OH resonance corresponds to 0.32 ± 0.16 equiv of water/mol of $[Cu(O\text{-}t\text{-}Bu)]_4$ consumed, which is very close to the amount expected from the isobutylene to *tert*-butyl alcohol ratio (ca. 0.26 equiv/mol of $[Cu(O\text{-}t\text{-}Bu)]_4$).

The conditions present in the static system differ in some respects from those characteristic of the dynamic system, and there is no guarantee that the same deposition mechanisms operate under both a static and dynamic vacuum. Nevertheless, it is reasonable to propose that the elimination mechanism in Figure 4 accurately describes how copper(I) oxide is formed from copper(I) *tert*-butoxide, especially since the same metal-containing and organic byproducts are observed under both conditions.

Deposition of Copper Metal. Whereas copper(I) oxide is the exclusive metal-containing product deposited from copper(I) *tert*-butoxide at 510 K, copper metal is deposited from copper *tert*-butoxide on silicon(100) or borosilicate glass at temperatures of 670 K. The deposits exhibit sharp powder X-ray diffraction profiles characteristic of copper metal. The deposits are polycrystalline, and there is no evidence of either oriented or epitaxial growth. Auger depth profile analyses confirm the presence of copper and indicate that the interiors of the deposits contain ~2% oxygen and no carbon (Figure 5). SEM images show that the films consist of roughly surfaced spherical islands ~0.75 μm in diameter (Figure 6); the deposit thickness is on the order of 1 μm. The films are not electrically well-connected; this is often (but not always) the case for the deposition of copper on untreated silicon or silicon oxide substrates.

Organic Byproducts Formed during Copper Metal Deposition. The quadrupole mass spectrum of the gaseous byproducts formed during the deposition of copper metal in the dynamic system is similar to that obtained during the deposition of copper(I) oxide; specifically, only *tert*-butyl alcohol and isobutylene are detected. In the static vacuum apparatus with both the deposition zone and the precursor reservoir heated to 670 K, thermolysis of the precursor occurs over 6 h to form principally copper metal as shown by elemental analysis. Quantitative ^1H NMR spectroscopy shows that 1.18 ± 0.08 equiv of *tert*-butyl alcohol and 2.06 ± 0.08 equiv of isobutylene are formed per mole of $[Cu(O\text{-}t\text{-}Bu)]_4$ consumed. No other organic products were evident. The larger isobutylene to *tert*-butyl alcohol ratio at 670 vs 510 K probably arises from different temperature dependences of the rates of proton transfer vs elimination of isobutylene from the surface *tert*-butoxide groups; i.e., isobutylene elimination is slightly faster than proton transfer at higher temperatures.

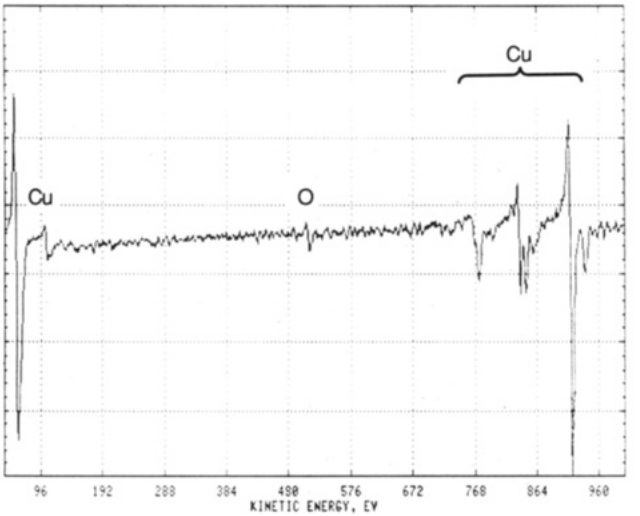

Figure 5. Auger spectrum of copper metal deposit on Si(100) obtained from $[Cu(O\text{-}t\text{-}Bu)]_4$ at 670 K.

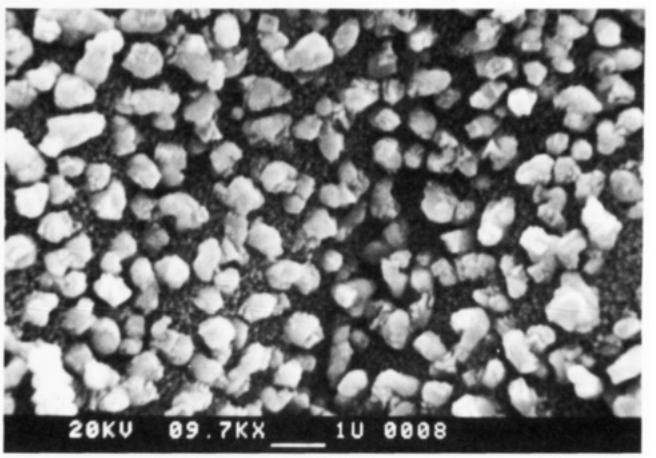

Figure 6. SEM micrograph at 15 kV showing island structure of copper deposit obtained from $[Cu(O\text{-}t\text{-}Bu)]_4$ at 670 K.

Mechanism of Copper Metal Deposition. Several mechanisms could account for the formation of copper metal from copper(I) *tert*-butoxide. One possibility is a radical mechanism in which the copper–oxygen bonds of $[Cu(O\text{-}t\text{-}Bu)]_4$ cleave to give *tert*-butoxy radicals (eq 6).

$$[CuOC(CH_3)_3]_4 \rightarrow 4Cu + 4{\cdot}OC(CH_3)_3 \quad (6)$$

This mechanism can be ruled out immediately, however, since *tert*-butoxy radicals are known to give acetone,[53]

(53) Batt, L.; Benson, S. W. *J. Chem. Phys.* **1962**, *36*, 895–901.

which is *not* one of the organic species formed during deposition.

It is more likely that the mechanism of copper deposition at 670 K is closely related to the mechanism of copper(I) oxide deposition at 510 K, especially in view of the very similar organic product distributions observed at the two temperatures. In particular, we propose that at 670 K the surface-bound *tert*-butoxide groups undergo the same elimination processes that operate at lower temperatures to give copper(I) oxide but that the latter product converts rapidly at 670 K to give copper metal.

At least two different pathways for the conversion of copper(I) oxide to copper metal may be envisaged. One of these involves the reduction of copper(I) oxide by isobutylene (eq 7), but this possibility can be ruled out be-

$$2Cu_2O + CH_2{=}C(CH_3)_2 \rightarrow 4Cu + CH_2{=}C(CH_3)CHO + H_2O \quad (7)$$

cause no isobutylene oxidation products such as aldehydes or carboxylic acids are detected.[54,55] The more likely pathway involves the conversion of copper(I) oxide to copper metal by direct deoxygenation to give O_2 (eq 8). At

$$Cu_2O \rightarrow 2Cu + \tfrac{1}{2}O_2 \quad (8)$$

first glance, this mechanism does not seem to be a plausible one for the formation of copper metal because the equilibrium pressure of oxygen over copper(I) oxide has been reported to be 10^{-17} Torr at 670 K.[56] There are a few claims, however, that copper(I) oxide undergoes deoxygenation at temperatures as low as 570 K.[57-60]

We have tested whether a deoxygenation mechanism is operative by heating a MOCVD-grown deposit of copper(I) oxide whiskers at 670 K under dynamic vacuum for 1 week. X-ray powder diffraction data before and after heating indicate that a significant fraction (~80%) of the copper(I) oxide present in the deposit converts to copper metal over this period. Although the time frame for this experiment is longer than that of a typical MOCVD deposition, oxygen loss is expected to be slower from a bulk sample than from the surface layer of a growing MOCVD deposit. Evidently, deoxygenation of high-surface-area copper(I) oxide is relatively facile even at temperatures as low as 670 K.[61]

Attempts were made to detect and quantify the O_2 that this Cu_2O to Cu deoxygenation process should yield. Unfortunately, the small amounts of oxygen produced and the presence of oxygen as a background contaminant makes it difficult to establish unambiguously whether O_2 is in fact a product of copper metal formation.

Ultrahigh-Vacuum Studies on Cu(111) Single Crystals. Although the static vacuum experiments provide information about the product distributions, they do not provide any *direct* evidence of the intermediate species present during deposition and the dynamic processes they undergo. Accordingly, we have carried out direct spectroscopic studies of these chemical processes using surface analytical techniques.

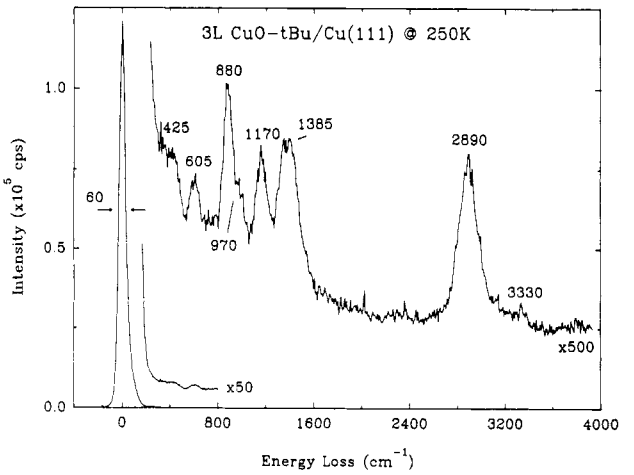

Figure 7. EELS spectrum of Cu(111) single crystal surface dosed with 0.24 langmuir of $[Cu(O\text{-}t\text{-}Bu)]_4$ at 250 K.

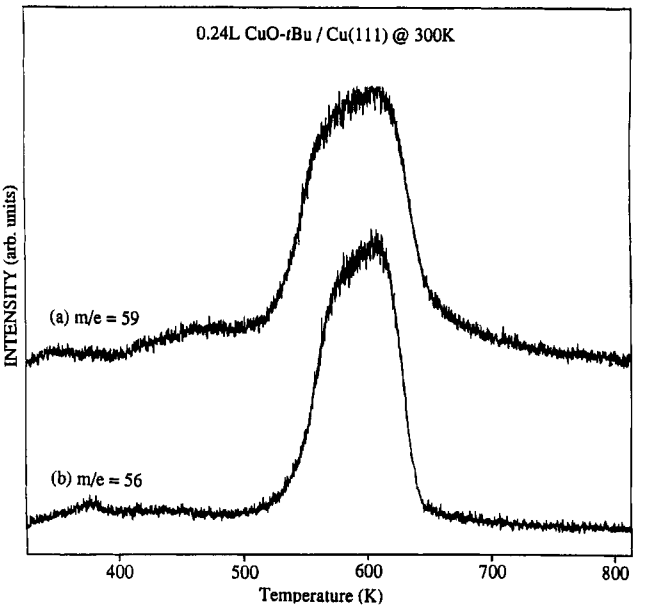

Figure 8. TPD profiles at 2 K/s of (a) *tert*-butyl alcohol and (b) isobutylene produced from a Cu(111) single crystal dosed with 0.24 langmuir of $[Cu(O\text{-}t\text{-}Bu)]_4$ at 300 K.

A Cu(111) single-crystal surface was dosed with approximately 0.24 langmuir of copper(I) *tert*-butoxide at 250 K. High-resolution electron energy loss spectra (EELS) of the dosed surface clearly reveal the presence of *tert*-butoxide groups: peaks were noted at 605 (Cu–O stretch), 880 (C–O stretch), 1170 (CH_3 rock), 1385 (CH_3 deformation), and 2890 cm^{-1} (C–H stretch) (Figure 7) which are consistent with the peaks at 600, 920, 940, 1180, 1355, and 1380 cm^{-1} in the infrared spectrum of the precursor. The decrease in the C–O stretching frequencies of the *tert*-butoxy groups from 920 and 940 cm^{-1} in the precursor to 880 cm^{-1} on the Cu(111) surface suggests that upon adsorption there is some structural change involving the copper core of $[Cu(O\text{-}t\text{-}Bu)]_4$. Nevertheless, it is clear that the *tert*-butoxy groups themselves remain essentially intact.

Temperature-programmed desorption (TPD) studies (Figure 8) show that fragmentation of the *tert*-butoxide groups and desorption of *tert*-butyl alcohol (m/e = 59) and isobutylene (m/e = 56) occur upon heating the surface to between 550 and 650 K (T_{max} = 610 K). The identification of these species was confirmed by integrated desorption

(54) Zhiznevskii, V. M.; Fedevich, E. V. *Kinet. Catal. (Engl. Transl.)* **1971**, *12*, 1073–1077.
(55) Kister, A. T. Belg. Patent 618,223, 1962; *Chem. Abstr.* **1963**, *59*, 5024f.
(56) Lustman, B. *Steel Processing* **1946**, 669–676.
(57) Maiti, G. C.; Ghosh, S. K. *Fertilizer Technol.* **1983**, *20*, 58–59.
(58) Seidl, R.; Strelka, V. *Czech. J. Phys.* **1959**, *9*, 757.
(59) Zhao, L. *Wuli Huaxue Xuebao*, **1987**, *3*, 570–572; *Chem. Abstr.* **1988**, *108*, 80144m.
(60) In addition, there are several studies of the reverse process, the low-temperature oxygenation of copper. Dubois, L. H. *Surf. Sci.* **1982**, *119*, 399–410 and references therein.
(61) The intermediacy of phases whose bulk form is kinetically stable may also be important in other MOCVD processes. We have evidence that that deposition of silver films from fluorinated silver-containing precursors proceeds via a silver(I) fluoride intermediate phase. Jeffries, P. M.; Girolami, G. S. *J. Organomet. Chem.*, in press.

mass spectrometry. All of these products are formed simultaneously, and since neither *tert*-butyl alcohol nor isobutylene bind to Cu(111) at these temperatures, the desorption of these species must be limited by the rate of the *tert*-butoxide fragmentation process.

The mechanism that we have proposed for the generation of Cu_2O from $[Cu(O\text{-}t\text{-}Bu)]_4$ involves surface hydroxide intermediates (Figure 4). Significantly, surface hydroxyl species *can* be detected by EELS as fragmentation of the *tert*-butoxide groups commences: a weak feature at 3330 cm^{-1} (O–H stretch) is observed. All of the TPD and EELS data are consistent with the elimination mechanism proposed in Figure 4, with the elimination of isobutylene being rate limiting.

An Auger spectrum taken after the dosed surface had been heated to 900 K showed the surface to be free of carbon and oxygen. This demonstrates that the generation of copper metal from $[Cu(O\text{-}t\text{-}Bu)]_4$ is a relatively clean process, a result which is consistent with the purity of the bulk films generated under MOCVD conditions.

These results are similar to those reported by Brainard and Madix for the reaction of *tert*-butyl alcohol with an oxidized Cu(110) surface.[62] These workers showed that this reaction yields surface-bound *tert*-butoxide groups, which fragment upon heating to 600 K to give isobutylene, *tert*-butyl alcohol, and water. Depending on the degree of oxidation of the copper(110) surface, they found activation energies of 32–40 kcal/mol and preexponential factors of 10^{12}–10^{15} s^{-1} for this elimination process; a deuterium kinetic isotope effect at 575 K of $k_H/k_D = 2.3$ was also determined. These activation parameters are consistent with the TPD results we have obtained upon heating Cu(111) surfaces dosed with $[Cu(O\text{-}t\text{-}Bu)]_4$.

Discussion of the Results in our Preliminary Communication. The possible role of water in the mechanism of formation of Cu_2O from $[Cu(O\text{-}t\text{-}Bu)]_4$ was discussed in our preliminary communication,[38] and two points raised in that paper require comment. First, although we originally suggested that the stoichiometry of the deposit obtained (Cu vs Cu_2O) was dependent on whether or not water was present during deposition, our more complete results clearly demonstrate that this suggestion was incorrect and that the stoichiometry obtained is dependent only on the *temperature* of the deposition. Second, we carried out a deposition of Cu_2O in the presence of D_2O, and found that deuterium labels were incorporated into the *tert*-butyl alcohol byproduct. We interpreted this result to mean that *either* the hydrolysis/dehydration pathway (eqs 1 and 2) was the mechanism by which copper(I) oxide was formed from $[Cu(O\text{-}t\text{-}Bu)]_4$ *or* that incorporation of deuterium labels in the *tert*-butyl alcohol product was occurring after deposition was complete. It is now clear that this latter possibility is the correct one, and that formation of copper(I) oxide occurs not by a hydrolysis/dehydration pathway but by a different mechanism (Figure 4).

Concluding Remarks. $[Cu(O\text{-}t\text{-}Bu)]_4$ has the interesting property of giving deposits of either copper(I) oxide or copper metal depending on the deposition temperature. The study of the deposition mechanism has afforded interesting mechanistic insights into the MOCVD processes. The deposition of copper(I) oxide from copper(I) *tert*-butoxide occurs at 510 K via an elimination mechanism involving loss of isobutylene from *tert*-butoxide groups to give surface hydroxyl species. Subsequent proton transfer processes yield *tert*-butyl alcohol, water, and copper(I) oxide. The deposition of copper metal from copper(I) *tert*-butoxide at 670 K apparently occurs by the same mechanism, but the copper(I) oxide phase initially formed deoxygenates to give copper metal as the film grows.

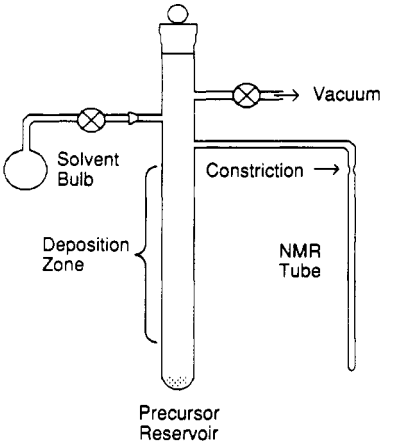

Figure 9. Schematic diagram of static vacuum apparatus.

The role of copper(I) oxide as an intermediate in the growth of copper metal films from $[Cu(O\text{-}t\text{-}Bu)]_4$ demonstrates an important point: MOCVD-grown films of pure metals can sometimes be produced via intermediate oxide phases whose bulk form is kinetically *stable* under the deposition conditions. This situation can arise if the intermediate oxide phase readily undergoes surface deoxygenation but bulk oxygen atom diffusion processes are slow. Specifically, if surface deoxygenation of copper(I) oxide is fast compared to the MOCVD deposition rate, then bulk oxygen atom diffusion is unnecessary and a copper metal deposit will be obtained. Thus the stability of a bulk phase cannot necessarily be used to rule out the possibility that it is an intermediate in a MOCVD growth mechanism.[63]

Experimental Section

Auger spectra were recorded on a Physical Electronics 595 system with a beam energy of 3 kV and a beam current of ca. 5 μA. X-ray photoelectron spectra were induced by a 15-kV, 400-W Mg Kα radiation source (1253.6 eV) on a Perkin-Elmer 5400 ESCA/Auger system. Spectra were obtained with a pass energy of 89.45 eV and an energy resolution of 0.5 eV/step. Auger and XPS spectra were collected after the samples had been argon ion sputtered to remove surface contamination. X-ray powder diffraction data were recorded on a Rigaku D-Max instrument. Scanning electron micrographs were obtained on a ISI DS-130 microscope. The NMR data were recorded on a General Electric QE-300 spectrometer at 300 MHz. Chemical shifts are reported in δ units (positive chemical shifts to higher frequency) relative to $SiMe_4$. Microanalyses were performed by the University of Illinois Microanalytical Laboratory. $[Cu(O\text{-}t\text{-}Bu)]_4$ was prepared according to a published procedure.[64]

Dynamic Vacuum MOCVD Apparatus. The dynamic vacuum system used to deposit the films and to provide qualitative information about the byproduct gases produced during the deposition has been described elsewhere.[65] Two methods were employed to heat the deposition zone: external heating with a tube furnace and internal heating with a hot stage. With external heating, there is a linear temperature gradient in the hot zone.

(62) Brainard, R. L.; Madix, R. J. *Surf. Sci.* **1989**, *214*, 396–406.

(63) The formation of oxygen as a byproduct of copper deposition may explain the relatively low recovery of carbon in the static system experiments to produce copper metal. At the higher temperatures and in the presence of some oxygen, partial combustion of the hydrocarbon byproducts could occur to produce CO_2 and CO which would not be detected by ^1H NMR spectroscopy.

(64) Tsuda, T.; Hashimoto, T.; Saegusa, T. *J. Am. Chem. Soc.* **1972**, *94*, 658–659.

(65) Girolami, G. S.; Jensen, J. A.; Gozum, J. E.; Pollina, D. M. *Mater. Res. Soc. Symp. Proc.* **1988**, *121*, 429–438.

For example, with the center of the hot zone set at a temperature of 670 K, the temperature at either end of the 30-cm tube furnace is 500 K. The internal hot stage is able to keep the temperature of the substrates more nearly uniform. The precursor was sublimed at 380 K, and the tube furnace or hot stage was maintained at 510 for deposition of copper(I) oxide and at 670 K for deposition of copper metal. The films were deposited over ~36 h from ~0.5 g of precursor.

Static Vacuum Apparatus. The static vacuum apparatus (Figure 9) provides quantiative information about the byproduct gases produced during the deposition. The main parts of the apparatus are the precursor reservoir, the solvent bulb, the deposition zone, and the NMR tube. The solvent bulb was charged with a benzene/benzene-d_6 solvent mixture. This mixture was degassed with three freeze–pump–thaw cycles. The stopcock between the solvent bulb and the rest of the apparatus was then closed. The precursor reservoir was charged with $[Cu(O\text{-}t\text{-}Bu)]_4$ and the apparatus was evacuated to $\sim 10^{-5}$ Torr. The stopcock between the apparatus and the vacuum pump was then closed and the apparatus was left under a static vacuum for the duration of the procedure. The NMR tube was cooled to 77 K, and the deposition zone and precursor reservoir were heated to the appropriate temperatures. After decomposition was complete, the apparatus was allowed to cool. The stopcock to the solvent bulb was opened and the solvent mixture was condensed into the NMR tube quantitatively. The NMR tube was then flame sealed at the constriction.

After the proton T_1 relaxation times were measured, a ^1H NMR spectrum of the sample was collected with a preacquisition delay of at least $5T_1$ between acquisitions to insure a quantitative measurement. The longest T_1 relaxation time was typically 35–40 s. From the amount of benzene used, the proton concentration of the solvent, and the relative intensities of the NMR peaks, the amounts of byproduct gases trapped during the deposition were calculated.

The proton concentration of the solvent was determined by placing some of the solvent mixture in a NMR tube and then weighing the tube. A small amount of *tert*-butyl alcohol was then added to the tube and the tube was again weighed. The ^1H NMR spectrum was then obtained as previously described. From the amount of solvent mixture used, the amount of *tert*-butyl alcohol used, and the relative intensities of the NMR peaks, the proton concentration of the solvent was calculated.

Static Vacuum Analysis of Byproducts. For the formation of copper(I) oxide, the deposition zone and precursor reservoir were heated to 510 and 380 K, respectively, for 12 h. $[Cu(O\text{-}t\text{-}Bu)]_4$ (0.210 g, 3.84×10^{-4} mol) and 0.53 g of the benzene/benzene solvent mixture (2.35×10^{-3} mol of H/g of solvent) were used. The relative intensities of the C_6H_6 (δ 7.27), $(CH_3)_3COH$ (δ 1.09), $(CH_3)_3COH$ (δ 3.00), $(CH_3)_2CCH_2$ (δ 1.59), and $(CH_3)_2CCH_2$ (δ 4.74) peaks were 1.00:4.61:0.71:3.95:1.35, respectively; thus 6.4×10^{-4} mol of *tert*-butyl alcohol, 8.2×10^{-4} mol of isobutylene, and 1.2×10^{-4} mol of water were present. The amount of *tert*-butyl alcohol and isobutylene detected accounts for 95% of the carbon originally in the precursor. A microanalysis of the solid deposit showed it to consist largely of Cu_2O. (Found: Cu, 87.3; C, 1.30; H, 0.33. Calcd for Cu_2O: Cu, 88.8.) The X-ray powder diffraction profile of the deposit contained broad peaks at the proper d spacings for copper(I) oxide.

For the formation of copper metal, the deposition zone and precursor reservoir were both heated to 670 K for 6 h. $[Cu(O\text{-}t\text{-}Bu)]_4$ (0.218 g, 3.99×10^{-4} mol) and 0.58 g of the benzene/benzene-d_6 solvent mixture (9.49×10^{-3} mol of H/g of solvent) were used. The relative intensities of the C_6H_6, $(CH_3)_3COH$, $(CH_3)_3COH$, $(CH_3)_2CCH_2$, and $(CH_3)_2CCH_2$ peaks were 1.00:0.761:0.111:0.894:0.309, respectively; thus 4.7×10^{-4} mol of *tert*-butyl alcohol, 8.2×10^{-4} mol of isobutylene, and 0.7×10^{-4} mol of water were formed. The amount of *tert*-butyl alcohol and isobutylene detected account for 81% of the carbon originally in the precursor. A microanalysis of the solid deposit showed it to consist largely of Cu. (Found: Cu, 97.29; C, 0.39; H, <0.01.)

***tert*-Butyl Alcohol Dehydration Control Experiments.** In the dynamic system, copper(I) oxide and copper metal were deposited as in a typical MOCVD experiment except the pretrap was not cooled. After deposition was complete, the system was heated for 24 h to ensure that all *tert*-butyl alcohol and isobutylene produced during the deposition was removed. The pretrap was cooled to 77 K and *tert*-butyl alcohol was passed over the heated deposits at the deposition temperatures. The material exiting the hot zone was analyzed in situ by a quadrupole mass spectrometer located just downstream of the hot zone, and no isobutylene was detected. The pretrap was then warmed to room temperature and again no isobutylene was detected by the quadrupole mass spectrometer.

In the static system, copper(I) oxide and copper metal were deposited with the apparatus open to vacuum and the NMR tube at room temperature. After the deposition was complete, the stopcock to the vacuum was closed, and *tert*-butyl alcohol was admitted from a bulb connected to the top joint of the apparatus into the heated system for 30 s. The NMR tube was then cooled to 77 K, the apparatus was cooled to room temperature, the deuterated solvent was collected in the NMR tube. The tube was flame sealed and its contents were analyzed by ^1H NMR spectroscopy. No isobutylene was detected.

Ultrahigh Vacuum Studies. Experiments were performed in a diffusion and titanium sublimation pumped ultrahigh vacuum chamber with a base pressure near 1×10^{-10} Torr. The system was equipped with four-grid low-energy electron diffraction optics (Varian), a single-pass cylindrical mirror analyzer (Physical Electronics) for Auger electron spectroscopy, a differentially pumped quadrupole mass spectrometer (Vacuum Generators) for temperature-programmed desorption, and a high-resolution electron energy loss spectrometer (McAllister Technical Services). For the EELS experiments, the angle of the incident electron beam (60° to the surface normal) and its energy (4–5 eV) were held constant and electrons were collected only in the specular direction. The elastic scattering peak from an adsorbate covered surface had an intensity of $>10^5$ cps and a full width at half maximum of 6–8 meV (50–60 cm^{-1}). For the TPD and integrated desorption mass spectrometry[66] experiments the heating rate was 2 K/s.

A 1-cm-diameter Cu(111) single-crystal disk (>99.999%, Monocrystals) was oriented, cut, and polished using standard techniques. The sample was mounted on a small, temperature-controlled molybdenum block which could be heated to over 1200 K by a tungsten filament or cooled to less than 100 K via copper braids attached to a liquid nitrogen reservoir. Temperatures were measured using a chromel–alumel thermocouple inserted into the side of the copper substrate. The crystal was cleaned of trace carbon, sulfur, and oxygen impurities by repeated cycles of neon ion sputtering (1000 eV, 8–10 $\mu A/cm^2$) at both 300 and 970 K followed by annealing in vacuum at 970 K. Sample cleanliness and order were carefully monitored using AES and LEED, respectively. The sample was sputtered and annealed before each experiment. $[Cu(O\text{-}t\text{-}Bu)]_4$ was introduced into the chamber through a heated, effusive molecular beam doser.

Acknowledgment. We thank the Department of Energy (Contract DEFG02-91 ER45439) for support of this work. Auger, XPS, and XPD were carried out in the Center for Microanalysis of Materials, University of Illinois, which is supported by the Department of Energy under the same contract. Scanning electron microscopy was performed at the Center for Electron Microscopy at the University of Illinois. P.M.J is the recipient of a University of Illinois Department of Chemistry Fellowship. G.S.G. is the recipient of an A. P. Sloan Foundation Research Fellowship and a Henry and Camille Dreyfus Teacher–Scholar Award.

Registry No. Cu_2O, 1317-39-1; Cu 98,O 2, 143903-07-5; copper *tert*-butoxide, 35342-67-7.

(66) Dubois, L. H. *Rev. Sci. Instrum.* **1989**, *60*, 410–413.